Tatinati S, Nazarpour K, Ang WT, Veluvolu KC. Multi-dimensional modeling of physiological tremor for active compensation in hand-held surgical robotics. *IEEE Transactions on Industrial Electronics* 2017, 64(2), 1645-1655.

DOI link to article:

http://dx.doi.org/10.1109/TIE.2016.2597119

Date deposited:

17/01/2017

Multi-Dimensional Modeling of Physiological Tremor for Active Compensation in Hand-Held Surgical Robotics

Sivanagaraja Tatinati,[1], Kianoush Nazarpour,[2], Wei Tech Ang, and [3], and Kalyana C. Veluvolu*[4]

[1] Sivanagaraja Tatinati is with School of Electronics Engineering, College of IT Engineering, Kyungpook National University, Daegu, South Korea 702-701.
[2]K. Nazarpour is with the School of Electrical and Electronic Enineering and the Institute of Neuroscience, Newcastle University, Newcastle, NE17RU, U.K.
[3]W. T. Ang is with School of Mechanical and Aerospace Engineering, Nanyang Technological University, Singapore.
[4]Kalyana C. Veluvolu (Corresponding author, e-mail: veluvolu@ee.knu.ac.kr) is with School of Electronics Engineering, College of IT Engineering, Kyungpook National University, Daegu, South Korea 702-701 and School of Mechanical and Aerospace Engineering, Nanyang Technological University, Singapore.

November 28, 2016

Abstract

Precision, robustness, dexterity, and intelligence are the design indices for current generation surgical robotics. To augment the required precision and dexterity into normal micro-surgical work-flow, hand-held robotic instruments are developed to compensate physiological tremor in real-time. The hardware (sensors and actuators) and software (causal linear filters) employed for tremor identification and filtering introduces time-varying unknown phase-delay that adversely affects the device performance. The current techniques that focus on three-dimensions (3D) tip position control involves modeling and canceling the tremor in three axes (*x, y*, and *z* axes) separately. Our analysis with the tremor recorded from surgeons and novice subjects shows that there exists significant correlation in tremor across the dimensions. Based on this, a new multi-dimensional modeling approach based on extreme learning machines (ELM) is proposed in this paper to correct the phase delay and to accurately model 3D tremor simultaneously. Proposed method is evaluated through both simulations and experiments. Comparison with the state-of-the art techniques highlight the suitability and better performance of the proposed approach for tremor compensation in hand-held surgical robotics.

*This research was supported by the Basic Science Research Program through the National Research Foundation of Korea (NRF) funded by the Ministry of Education, Science and Technology under the Grant NRF-2014R1A1A2A10056145.

1 Introduction

Physiological tremor is a major impediment to perform delicate and fine motor tasks, such as microsurgery [1, 2]. In microsurgical procedures, the surgeons hand motion must be precise at the magnitude smaller than few micrometers (10 μm) [1]. Even under normal conditions, physiological tremor exists in normal human motions to some degree with amplitude of approximately 100 μm [2, 3], and it adversely affects the outcome of the microsurgery. Consequently, surgical robots are being developed to provide surgeons with the required precision and dexterity to execute the microsurgical procedures successfully. Over the past two decades, the surgical robotics have evolved from autonomous robots to tele-operating robots and now to hand-held robotic instruments [4, 5]. For these surgical robotic instruments precision, dexterity, and intelligence form the design indices.

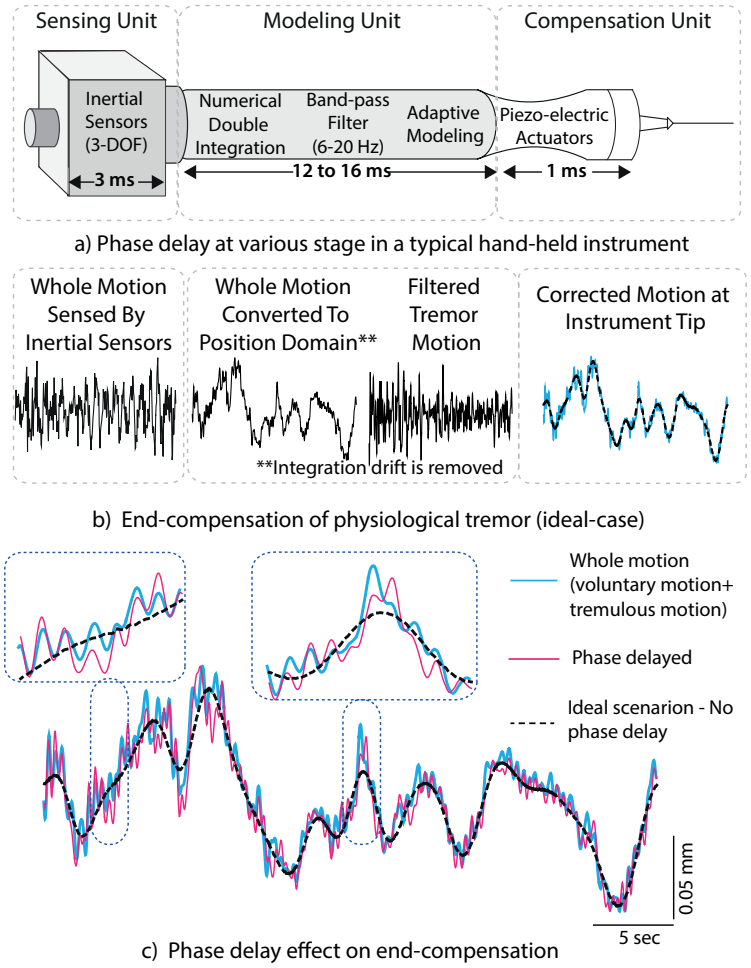

Figure 1: Active physiological tremor compensation and effect of phase delay

The advent of hand-held instruments has created an opportunity to augment the required precision and dexterity into the normal surgical work-flow by compensating the tremulous motion [6, 7]. The working principle of a typical hand-held instruments is simple as shown in Fig. 1 and it involves subsequent execution of three steps 1) sensing its own motion, 2) filtering the involuntary motion from the sensed motion, and 3) actuate the surgical end-effectors (instrument tip) based

on the filtered involuntary motions to compensate the erroneous motions. To possesses the advantages of being compact, multi-dimensional freedom as conventional surgical instrument, and less obstructive to manipulate, the hand-held instruments are embodied with miniature MEMS based inertial sensors to sense its own motion in three-dimensions (sensing unit) and piezo-electric actuators to manipulate the instrument end-effector (compensation unit), as shown in Fig. 1 [6, 7]. The intelligence to identify, filter and accurately model the involuntary motions from the whole sensed motion is provided by the adaptive signal modeling unit (modeling unit) [7, 8]. Furthermore, this unit generates the control signal for the three-dimensional (3D) tip motion to compensate tremor (compensating unit) based on the modeled tremor motion. For effective tremor compensation, all the above three stages have to be executed in one cycle (sample period) [7].

The voluntary hand motions during microsurgery are often superimposed with the involuntary motions such as physiological tremor, drift, noise and chorea etc. The meticulous nature of the microsurgical procedures restricts the voluntary movements to low frequency components i.e. less than 2 Hz [9]. Consequently, frequency selective linear filters have been employed to filter tremulous motion [10]. These linear filters serves also in removing the notorious numerical-integration drift due to double-integration and other unwanted noise/drift that comes from the sensing unit while converting the sensed motion in acceleration domain to position domain, as shown in Fig. 1. As physiological tremor lies in band of 6 Hz to 14Hz, the inherent phase-lag as small as 10° ($20ms$) can generate an out-of-phase control signal for compensation unit and this exacerbates the tip motion at instrument end-effector rather than compensating it. To illustrate the effect of phase delay on the instrument's tip position control, comparison between the corrected tip obtained with actual tremulous motion and delayed tremulous motion (obtained as described in Section II) for a typical trial is shown in Fig. 1(c). The experiments conducted with hand-held instrument (Micro) showed that the phase delay of liner filtering stage limited the compensation accuracy to only 20% and also destabilized the eye-had feedback loop [11].

Various factors such as causality, resolution and response-time of sensors, phase delay, and drift also effect the real-time performance [7, 10]. It is now evident that phase-lag is the single major factor that adversely effects the end compensation accuracy [8]. In the sensing unit shown in Fig. 1, the presence of on-board low-pass filter in accelerometers introduces a phase delay of 3 ms. An additional delay of 1 ms is identified as the response time for piezo-electric actuators. As the band pass filter employed in the modeling unit introduces frequency dependent (unknown) delay of 12-16 ms, a total delay in the range of 16 - 20 ms is unavoidable from sensing to compensation in these hand-held instruments.

Adaptive filtering techniques [8] that rely on truncated Fourier series (band-limited multiple Fourier linear combiner (BMFLC) [12–15]) have been popular to model the tremulous motion without any phase delay. Recently, in [15], a quaternion version of WFLC (QWFLC) has been developed to model the tremulous motion in quaternion domain and empirically proven to be more effective than the real domain WFLC. Further, the method QWFLC also demonstrated the effectiveness of multi-dimensional coupling in accurate modeling of tremor compared to uni-dimensional WFLC. Although, these methods accurately model the tremulous motion, the study in [10] demonstrated that the unknown phase-delay introduced by the pre-filtering stage adversely effects the final outcome. Consequently, the design indices for the adaptive tremor modeling algorithms can be given as:

i) unknown phase-delay correction

ii) accurate tremor modeling

iii) less computational complexity.

To this end, Autoregressive (AR) methods [16], BMFLC and least squares-support vector machines (MWLS-SVM) [17] methods are customized to perform multi-step prediction of physiological tremor to counter the known and unknown phase delays. Among the existing methods, MWLS-SVM manages to meet all the indices, there is however much scope for improvement in terms of accurate modeling of unknown phase-delay and reducing the computational complexity. To date, all these existing methods consider the sensed motion in three-dimensions as three independent signals. To achieve 3D tremor estimation and compensation, the adaptive filtering method must be applied to all three axes separately. Hence a multi-dimensional approach that can better utilize the information from cross-channels to counter the unknown phase delay and provide more accurate 3D tremor is required.

Several popular signal processing methods like support vector machines (SVM) have been extended to multi-dimensional framework from the original single-dimensional framework [18]. The improved multi-dimensional framework however might suffer from either loss of generality or significant increase in computational complexity due to the lack of multi-dimensional modeling scheme in its cost function [19, 20]. It has been empirically proved that innate structure of single hidden layer feed-forward networks (SLFN) can provide multi-dimensional modeling simultaneously where each output node can serve as the modeled output for each dimension [21]. Extreme learning machines (ELMs) is one of the effective learning procedure to learn the SLFN parameters and has been successfully applied in solving regression, function estimation, and multi-class classification problems [19,21,22]. Further it is established that ELM has better generalization performance and less computational complexity [19–21].

Motivated by this, in this paper, we developed a unified multi-dimensional modeling approach with ELM which is capable of integrating the cross-dimension couplings, and simultaneously solve the phase delay correction and thereby provide more accurate 3D tremor modeling with less computational complexity. The cost function of conventional ELM does not have the multi-dimensional form. Consequently, it provides unequal penalty for all dimensions and it might effect the multi-dimensional modeling performance. To address this issues, a robust multi-dimensional ELM (md-RELM) that provides equal penalty for all dimensions is developed in this paper. Further, to adapt to the non-stationary characteristics of tremor, we also propose an online sequential update for the robust multi-dimensional ELM (OS-mdRELM). To quantify the suitability of the proposed multi-dimensional technique for tremor modeling, analysis was conducted on the tremor data collected from microsurgeons and novice subjects. The proposed technique is also validated experimentally with hand-held robotic instrument (iTrem). Results showed that the proposed multi-dimensional paradigm significantly improves the tremor modeling accuracy compared to the state-of-the-art modeling techniques.

In Section II, the proposed multi-dimensional tremor modeling approach with several ELM variants are discussed. Section III presents the performance evaluation of the proposed methods with tremor data. Discussions, future work, and conclusions are provided in Section IV and Section V respectively.

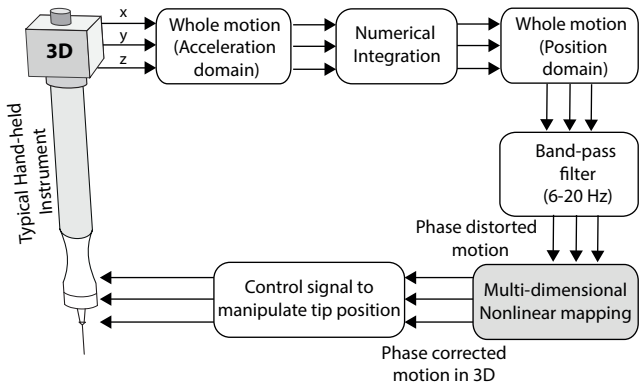

(a) Proposed multi-dimensional (3D) approach for delay correction

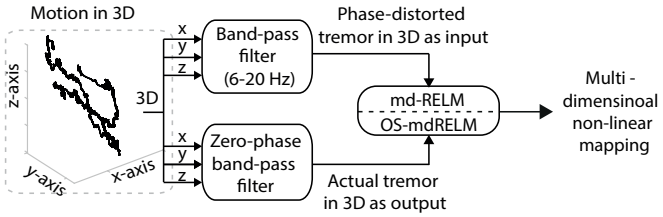

(b) Offline training for nonlinear mapping identification

Figure 2: Proposed unified approach for 3D tremor modeling

2 Methods and Materials

The main objective of this work is to develop a unified-framework that can effectively solve the phase-delay correction and provide more accurate 3D tremor estimation. In what follows, we shall discuss on how these challenges are addressed in this paper:

i) *Phase delay correction*: Unknown and time-varying- frequency dependent delay in the range of 16 to 20 ms is inevitable due to the presence of various linear filters at different stages in the signal processing chain. This delay correction problem is considered as a classical learning problem of estimating an unknown relation between the elements of an input space ($\mathbf{S} \in \mathcal{R}^m$) and elements of an outer space ($\mathbf{T} \in \mathcal{R}^n$), as shown in Fig. 2(b). The elements of input space are the phase-distorted tremulous motion components obtained after conventional band-pass filter and the elements of output space are the actual tremulous motion components obtained with a zero-phase band-pass filter. In this work, we adopt extreme learning machines (ELM) to identify a generalized and accurate $inverse - mapping$ nonlinear function ($\boldsymbol{\beta}(\cdot)$) such that $\boldsymbol{\beta}(\mathbf{s} \in \mathbf{S}) \approx t \in T$.

ii) *3D tremor modeling*: By the very nature, the single-dimensional modeling techniques lack the structure to utilize the cross-dimensional coupling information. By its inherent structure, the learning method ELM is capable of integrating the cross-dimension couplings. To simultaneously also solve the phase delay correction with the $inverse - mapping$ function, a robust multi-dimensional modeling based on ELM is developed.

iii) *Computational complexity*: The innate structure of ELM facilitates modeling of tremor in three dimensions simultaneously. Therefore, the computational power required to achieve 3D tremor modeling can be significantly reduced with the proposed multi-dimensional approach compared to that of conventional single-dimensional approach. Furthermore, it has been rigorously

proved that the computational requirement of ELM is very small compared to other popular machine learning techniques such as SVM [19, 21].

In the following, we first discuss the proposed multi-dimensional learning techniques based on ELM for 3D tremor modeling. Conventional ELM can be trained to perform multi-dimensional modeling of tremulous motion. However, the output layer weights of the trained network lacks the technique to uniformly penalize the cross-dimension couplings of all dimensions [19]. Further, the cross-dimension coupling might contain outliers or irrelevant information for modeling [20]. To address these issues, we customized ELM and its cost function to suit to our 3D tremor estimation problem and named as robust multi-dimensional ELM (md-RELM). As the physiological tremor is non-stationary in nature, to adapt the regularized ELM output weights over the time, we also developed the online sequential learning technique for md-RELM, named as OS-mdRELM. In what follows, both these techniques are discussed.

2.1 Robust Multi-dimensional ELM (md-RELM)

For a set of $\tilde{N}$ independently and identically distributed samples $\mathcal{S} = \{(\mathbf{s}_i, \mathbf{t}_i)|\mathbf{s}_i \in \mathcal{R}^m,\ \mathbf{t}_i \in \mathcal{R}^n; i = 1,\ \cdots,\ \tilde{N}\}$ with $\mathbf{S} = [\mathbf{s}_1, \cdots, \mathbf{s}_{\tilde{N}}]$ as input vector, $\mathbf{T} = [\mathbf{t}_1, \cdots, \mathbf{t}_{\tilde{N}}]$ as its corresponding target vector. With the randomly initialized input weights $\mathbf{w}$, hidden layer bias $\mathbf{b}$ and the computed output layer weights $\hat{\boldsymbol{\beta}}$, and sigmoid activation function, the multi-dimensional output with conventional ELM can be given as:

$$\mathbf{o}_k = f(\boldsymbol{s}_k) = \sum_{i=1}^{L} \hat{\boldsymbol{\beta}} g_i(\mathbf{w}_i \mathbf{s}_k + b_i) \tag{1}$$

The ouput weight matix ($\hat{\boldsymbol{\beta}}$) can be obtained with:

$$\hat{\boldsymbol{\beta}} = \mathbf{G}^{\dagger}\mathbf{T} \tag{2}$$

where $\mathbf{G}^{\dagger}$ is Moore-Penrose generalized matrix inversion of $\mathbf{G}$. For more detailed description about ELM, refer to [21].

The robust multi-dimensional ELM (md-RELM) is structurally similar to the conventional ELM except the cost function. The regularized cost function of ELM which provides equal penalty for all dimensions can be formulated as:

$$\begin{aligned} \min_{\boldsymbol{\beta},\ \boldsymbol{\epsilon}} \quad & \sum_{j=1}^{n} \frac{1}{2}||\boldsymbol{\beta}_j||^2 + \sum_{j=1}^{n} \frac{1}{2}\mathbf{c}_j \sum_{i=1}^{N} \boldsymbol{\lambda}_{ij}||\epsilon_{ij}||^2 \\ \text{subject to} \quad & \mathbf{t}_{ij} - \boldsymbol{\beta}_j \mathbf{g}(\mathbf{s}_i) = \epsilon_{ij},\ i = 1, \ldots, N. \end{aligned} \tag{3}$$

where $\boldsymbol{\lambda}_j = diag\{\lambda_{i1}, \ldots, \lambda_{in}\}$ represents the robust weight parameters and obtained as

$$\lambda_{ij} = \begin{cases} 1 & |\epsilon_{ij}/\hat{s}| \leq \tilde{c}_1; \\ \frac{\tilde{c}_2 - |\epsilon_{ij}/\hat{s}|}{\tilde{c}_2 - \tilde{c}_1} & \tilde{c}_1 \leq |\epsilon_{ij}/\hat{s}| \leq \tilde{c}_2; \\ 10^{-4} & |\epsilon_{ij}/\hat{s}| > \tilde{c}_2. \end{cases}$$

with $\hat{s} = \frac{IQR(\mathbf{s}_i)}{2 \times 0.6745}$, IQR defines the interquartile range, $\tilde{c}_1 = 2.5$, and $\tilde{c}_2 = 3$ and $\boldsymbol{c} = [c_1, \ldots, c_n]$ represents the regularization parameter.

Based on the Karush-Kuhn-Tuker (KKT) theorem, to train ELM is equivalent of solving the following dual optimization problem, can be given as:

$$\begin{aligned}\mathcal{L}_D &= \sum_{j=1}^{n}\frac{1}{2}||\boldsymbol{\beta}_j||^2 + \sum_{j=1}^{n}\frac{1}{2}\mathbf{c}_j\sum_{i=1}^{N}\boldsymbol{\lambda}_{ij}||\epsilon_{ij}||^2 - \\ &\sum_{j=1}^{n}\sum_{i=1}^{N}\alpha_{ij}(\epsilon_{ij} - t_{ij} + \boldsymbol{\beta}_j\mathbf{g}(\mathbf{s}_i))\end{aligned} \tag{4}$$

where $\alpha_{ij};\ i = 1,\ \ldots,\ N$ and $j = 1,\ \ldots,\ n$ represents the Lagrangian parameters. By solving the KKT optimality conditions, we can get an estimate of output weights:

$$\hat{\boldsymbol{\beta}}_j = (\frac{\mathbf{I}}{\mathbf{c}_j} + \mathbf{G}^T\boldsymbol{\lambda}_j\mathbf{G})^{-1}\mathbf{G}^T\boldsymbol{\lambda}_j\mathbf{t}j \tag{5}$$

The output of the mdRELM with the estimated output weights from the regularized cost function can be given as:

$$\mathbf{o}_k = f(\boldsymbol{s}_k) = \sum_{j=1}^{n}\sum_{i=1}^{L}\hat{\boldsymbol{\beta}}_j g_i(\mathbf{w}_i\mathbf{s}_k + b_i) \tag{6}$$

2.2 Online Sequential md-RELM (OS-mdRELM)

For an initial training dataset $\mathbf{S}_0 = \{\mathbf{s}_i, \mathbf{t}_i\}_{i=1}^{N}$, the initial output weights of robust multi-dimensional ELM can be given as:

$$\tilde{\boldsymbol{\beta}}_{(0)} = \mathbf{K}_{(0)}\mathbf{G}_{(0)}^T\tilde{\boldsymbol{\lambda}}\mathbf{T}_{(0)} \tag{7}$$

by considering $\tilde{\boldsymbol{\beta}}_{(0)} = [\boldsymbol{\beta}_1, \ldots, \boldsymbol{\beta}_n]$, $\tilde{\boldsymbol{c}}_{(0)} = [\boldsymbol{c}_1, \ldots, \boldsymbol{c}_n]$, $\tilde{\boldsymbol{\lambda}}_{(0)} = [\boldsymbol{\lambda}_1, \ldots, \boldsymbol{\lambda}_n]$, and $\mathbf{K}_{(0)} = (\frac{I}{\tilde{\mathbf{c}}} + \mathbf{G}_{(0)}^T\tilde{\boldsymbol{\lambda}}_{(0)}\mathbf{G}_{(0)})^{-1}$. Assume now that there are n_0 new observations $\mathbf{S}_1 = \{\mathbf{s}_i, \mathbf{t}_i\}_{i=N+1}^{N+n_0}$. Then the output weights can be computed as:

$$\tilde{\boldsymbol{\beta}}_{(1)} = \mathbf{K}_{(1)}^{-1}\begin{pmatrix}\mathbf{G}_{(0)}\\ \mathbf{G}_{(1)}\end{pmatrix}^T\begin{pmatrix}\tilde{\boldsymbol{\lambda}}_{(0)} & 0\\ 0 & \tilde{\boldsymbol{\lambda}}_{(1)}\end{pmatrix}\begin{pmatrix}\mathbf{T}_{(0)}\\ \mathbf{T}_{(1)}\end{pmatrix} \tag{8}$$

where $\mathbf{K}_{(1)} = \left(\frac{I}{\mathbf{c}} + \begin{pmatrix}\mathbf{G}_{(0)}\\ \mathbf{G}_{(1)}\end{pmatrix}^T\begin{pmatrix}\tilde{\boldsymbol{\lambda}}_{(0)} & 0\\ 0 & \tilde{\boldsymbol{\lambda}}_{(1)}\end{pmatrix}\begin{pmatrix}\mathbf{G}_{(0)}\\ \mathbf{G}_{(1)}\end{pmatrix}\right)$.

By considering $\mathbf{K}_{(k)}^{-1} = \mathbf{P}_{(k)}$, we can generalize the relationship between $\tilde{\boldsymbol{\beta}}_{(k+1)}$ and $\tilde{\boldsymbol{\beta}}_{(k)}$ as [23]:

$$\tilde{\boldsymbol{\beta}}_{(k+1)} = \tilde{\boldsymbol{\beta}}_{(k)} - \mathbf{P}_{(k+1)}\mathbf{G}_{(k+1)}^T\tilde{\boldsymbol{\lambda}}_{(k+1)}(\tilde{\boldsymbol{\beta}}_{(k)}\mathbf{G}_{(k+1)} - \mathbf{T}_{(k+1)}) \tag{9}$$

where

$$\begin{aligned}\mathbf{P}_{(k+1)} &= \mathbf{P}_{(k)} - \mathbf{P}_{(k)}\mathbf{G}_{(k+1)}^T(\tilde{\boldsymbol{\lambda}}_{(k+1)}^{-1} + \\ &\mathbf{G}_{(k+1)}\mathbf{P}_{(k)}\mathbf{G}_{(k+1)}^T)^{-1}\mathbf{G}_{(k+1)}\mathbf{P}_{(k)}\end{aligned} \tag{10}$$

The output of the online sequential robust multi-dimensional ELM can be given as:

$$\mathbf{o}_k = f(\boldsymbol{s}_k) = \sum_{j=1}^{n}\sum_{k=1}^{L}\tilde{\boldsymbol{\beta}}_{(k+1),j}\mathbf{g}(\mathbf{s}_k) \tag{11}$$

2.3 Implementation of Multi-dimensional Tremor Modeling Approach

Functional block diagram representation for the proposed multi-dimensional approach (OS-mdRELM) is depicted in Fig. 3. In what follows, the step by step procedure for 3D estimation is itemized:

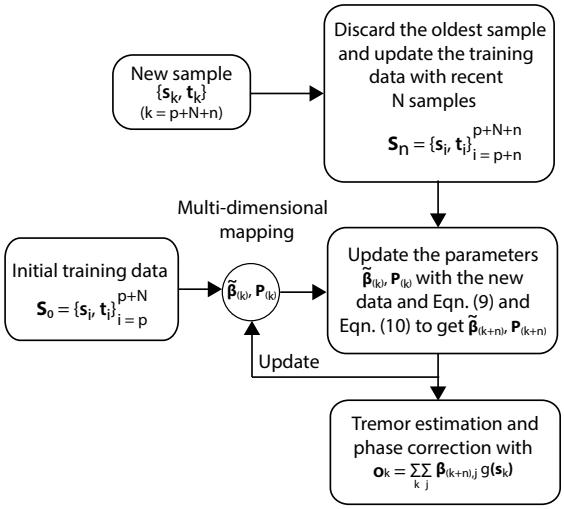

Figure 3: Functional block diagram representation for OS-mdRELM implementation

a) *Identification of non-linear inverse-mapping function ($\tilde{\boldsymbol{\beta}}_{(k)}$)*: To identify accurate yet generalized mapping, the first N samples of both delayed tremor motion and actual tremor motion in 3D are considered for the offline training, as shown in Fig. 2(b). In this training procedure, first the input vector is formulated in the embedded space constructed based on Taken's embedded theory [24, 25]. For three-dimensional modeling of tremor, the embedded space is formulated with the delayed *x, y,* and *z* axes. If two-dimensional modeling is considered, then the embedded space can be formulated with two delayed axes i.e, *x,* and *z* axes or *y,* and *z* axes. From this embedded space, md-RELM learns the non-linear *inverse-mapping* function ($\hat{\boldsymbol{\beta}}$) by utilizing the existence of cross-dimension coupling and with (5), as shown in Fig. 2(b).

b) *Updating the non-linear inverse-mapping function ($\tilde{\boldsymbol{\beta}}_{(k+n)}$)*: The non-linear mapping obtained with md-RELM can be updated in real-time with the arrival of every new sample by its online sequential learning approach (OS-mdRELM). First, upon arrival of the new sample for whole motion, the training database will be updated with the recent N samples by simply discarding the oldest sample in the data, as shown in Fig. 3. For example, assume that the training database has N samples i.e., from p to $p+N$ and the arrived new sample is $p+N+n$, then the training database will update to the recent N sample i.e., from $p+n$ to $p+N+n$. With the updated database and from Equations (10) and (9), the multi-dimensional nonlinear mapping will be updated to $\tilde{\beta}_{(k+n)}$. The phase delay correction will be carried out with (11). For OS-mdRLEM, this procedure will be repeated for every arrived new sample and accordingly the multi-dimensional mapping will be updated.

Finally, the tremor compensation framework with hand-held instruments is modified by incorporating the 'multi-dimensional modeling block' (comprises of the non-linear *inverse-mapping* function ($\tilde{\boldsymbol{\beta}}_{(k)}$)) after the band-pass filtering, as shown in Fig. 2(a). As a result, the phase delay induced by the filtering stage will be corrected and accurate 3D tremor estimation can be obtained.

3 Results

In this section, we first provide the details of physiological tremor data collected from microsurgeons and novice subjects. Later, the multi-dimensional correlation analysis and the comparison analysis are discussed, followed by the experimental validation of the proposed method.

3.1 Physiological Tremor Data Collection

Physiological tremor recordings were performed through the Micro Motion Sensing System ($M2S2$) and a sensorized stylus with reflector ball at its tip [26]. $M2S2$ provides a measurement in a $10 \times 10 \times 10\ mm^3$ workspace, with a resolution of 0.7 μm and minimum accuracy of 98% [7]. The 3D displacement of the reflector ball is calculated by using reflected Infrared rays from the ball and the photo sensitive diodes (PSDs). For more details about the design and data acquisition with $M2S2$, please refer [7, 26]. Two typical microsurigcal tasks are performed by 5 surgeons and 5 novice subjects [26]:

i) Pointing task: In this task, two dots were displayed on the monitor screen. One dot is white in color and fixed while the another dot is orange in color and will move according to the user's tool tip movement. The subjects were instructed to keep the orange dot overlapping the white dot for 30s.

ii) Tracing task: At the beginning of this task, a circle with 4 mm diameter was displayed on the monitor screen. The subjects were instructed to trace the circumference of the circle in clockwise direction as accurately as possible for 30s with the speed that is realistic for surgical manipulation tasks.

Each task was performed with three magnifications: 1x, 10x and 20x, and with grip force of 1 to 2 N. Sampling frequency of 250 Hz was employed. For more information about magnification and force conditions, see [26].

3.2 Performance Indices

Let $\mathbf{s}_x = [s_x(1), \cdots, s_x(k)]$, $\mathbf{s}_y = [s_y(1), \cdots, s_y(k)]$, and $\mathbf{s}_z = [s_z(1), \cdots, s_z(k)]$ represent the tremor signal of length k in x, y, and z axes respectively. In this work, the coupling between the tremor signal characteristics measured in multi-dimensions simultaneously is identified with correlation coefficients [24] and mutual information [25].

i) *Correlation coefficient*: The correlation coefficient (ρ) between any two axes can be defined as:

$$\rho_{xy} = \frac{\sum_{i=1}^{N}(s_x(i) - \mu_{\mathbf{s}_x})(s_y(i) - \mu_{\mathbf{s}_y})}{\sqrt{\sum_{i=1}^{N}(s_x(i) - \mu_{\mathbf{s}_x})^2 \sum_{i=1}^{N}(s_y(i) - \mu_{\mathbf{s}_y})^2}} \tag{12}$$

where $\mu_{\mathbf{s}_x} = \frac{1}{N}\sum_{i=1}^{N} s_x(i)$ and $\mu_{\mathbf{s}_y} = \frac{1}{N}\sum_{i=1}^{N} s_y(i)$ represent the mean values of $\mathbf{s}_x$ and $\mathbf{s}_y$.

ii) *Mutual Information*: The mutual information between any two axes can be defined as:

$$I(\mathbf{s}_x; \mathbf{s}_y) = H(\mathbf{s}_x) + H(\mathbf{s}_y) - H(\mathbf{s}_x; \mathbf{s}_y) \tag{13}$$

where $H(\mathbf{s}_x)$ and $H(\mathbf{s}_y)$ are the entropies of $\mathbf{s}_x$ and $\mathbf{s}_y$ respectively and $H(\mathbf{s}_x; \mathbf{s}_y)$ represents the joint differential of $\mathbf{s}_x$ and $\mathbf{s}_y$. If $\mathbf{s}_x$ and $\mathbf{s}_y$ are Gaussian random variables with variances σ_x^2 and σ_y^2 then $H(\mathbf{s}_x) = \frac{1}{2}[1 + log(2\pi\sigma_x^2)]$ and $H(\mathbf{s}_x; \mathbf{s}_y) = 1 + log(2\pi) + \frac{1}{2}log(\sigma_x^2\sigma_y^2(1 - \rho^2))$.

iii) *Accuracy*: The tremor modeling performance of all methods is quantified by using $\%Accuracy$, defined as:

$$\%Accuracy = \frac{RMS(s) - RMS(e)}{RMS(s)} \times 100; \tag{14}$$

where $RMS(s) = \sqrt{(\sum_{k=1}^{k=m}(s_k)^2/m)}$ with m is the number of samples, s_k is the input signal at instant k and e is the obtained estimation error with a method.

3.3 Cross-dimensional coupling analysis

The tremor data is pre-processed to analyze the cross-dimensions coupling. This pre-processing is an offline procedure and its main objective is to accurately separate the tremulous motion from the voluntary motions and other low-frequency components in the whole sensed motion. To this end, we employed a zero-phase third-order Butterworth band-pass filter with pass-band of 6 to 20 Hz. The processed tremor data was shortened to 29s to remove the transient effect due to the pre-filtering stage.

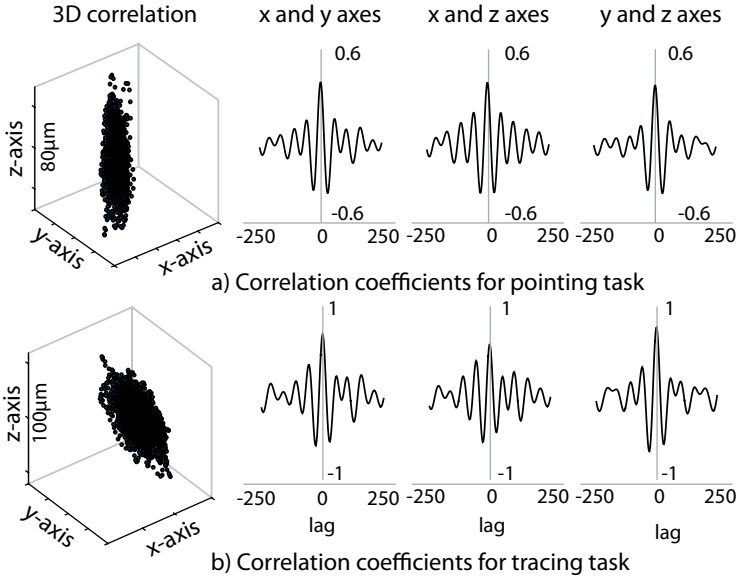

Figure 4: Correlation coefficients obtained for Subject #1

The correlation coefficients readily evaluates the linear relationship between across the channels. With the correlation coefficients (defined in (12)), we found that the tremor measurements in *x, y,* and *z* axes are not independent time series and there exists cross-dimensional correlation. For illustration, the correlation obtained between *x*-*y* axes, *x*-*z* axes, and *y*-*z* axes for subject #1 are shown in Fig. 4. For this subject, correlation coefficients 0.9, 0.65, and 0.86 are obtained for *x*-*y* axes, *x*-*z* axes, and *y*-*z* axes respectively for tracing task, whereas for the pointing task the correlation coefficients are 0.5, 0.43, and 0.36 for *x*-*y* axes, *x*-*z* axes, and *y*-*z* axes respectively. For all subjects and trials, statistical results shown in Fig. 5(a) reveal that there exists a significant level of cross-dimensions correlation.

As tracing task involves more control, larger correlation in tremor amplitude can be observed as compared to pointing task. To further evaluate the arbitrary coupling in cross-dimensions, we

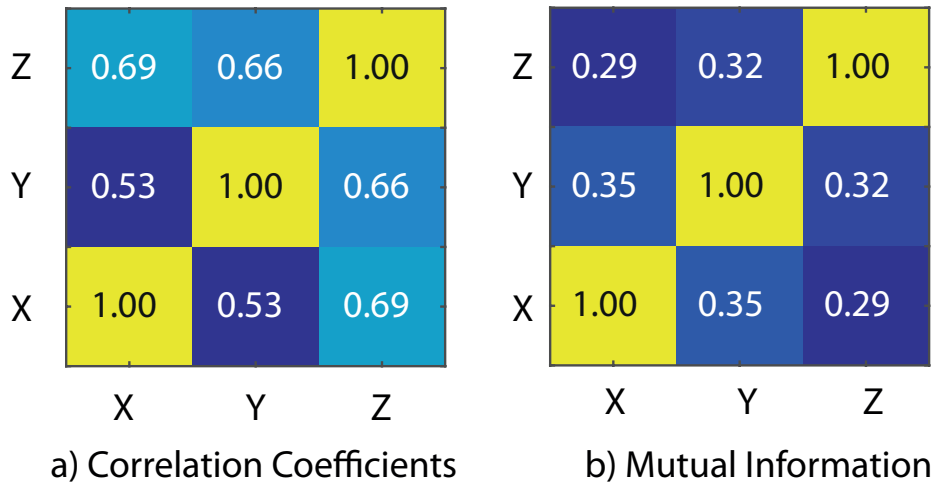

Figure 5: Cross-dimensional coupling analysis over all subjects and trials

analyzed the mutual information. This measure takes the nonlinear dependencies into consideration and then evaluates the arbitrary coupling across the dimensions. Furthermore, this measure is also independent to the transformations acting on the dimensions. The mutual information obtained across the dimensions on the whole data set is shown in Fig. 5(b). Results show that a normalized coupling of 0.35 and 0.29 exists between x - y axes and x - z axes respectively. These results are in line with the results obtained with the correlation coefficients.

3.4 Optimal Parameter Selection

The hyper-parameters of md-RELM that require optimal initialization are: 1) number of hidden neurons (L) in the hidden layer, 2) the embedded dimensions (m), and 3) regularization constant ($\mathbf{c}$). To identify the optimal initialization, we randomly chose ten trials per task. In each trial, first four seconds data (1000 samples) is considered as training dataset and the rest 25 seconds as the testing data set. We conducted a grid search on the chosen twenty trials with wide range of values for number of hidden neurons as $1 \leq L \leq 1000$, the embedded dimensions as $1 \leq m \leq 100$, and regularization constant as $10^0 \leq \mathbf{c} \leq 10^{10}$.

The md-RELM was trained (as shown in Fig. 2) with all possible combinations of L, m, and $\mathbf{c}$ on the training data set of each trial. The obtained non-linear mapping with each combination was later employed for modeling the testing data. For each combination, RMS of estimation error obtained according to (14) is computed. The triplet (L, $m, \mathbf{c}$) that provides the least RMS of estimation error was considered as the optimal parameter set for initialization. For illustration, the grid search conducted on a single trial with $\mathbf{c} = [10^3, 10^3, 10^3]$ for the complete of(L, m) is shown in Fig. 6(a). The RMS of error obtained for various selections of $\mathbf{c}$ in the chosen range also shown in Fig. 6(b). For this particular trial, the identified optimal initialization was $L = 171$, $m = 69$, and $\mathbf{c} = [10^3, 10^3, 10^3]$. Similar analysis for all trials does not show significant variations in the identified parameter set. Thus, for all subjects, we choose parameters as $L = 171$, $m = 69$, and $\mathbf{c} = [10^3, 10^3, 10^3]$. Same parameters were selected for conventional ELM. For the case of MWLS-SVM, we employed the parameter set reported in [17].

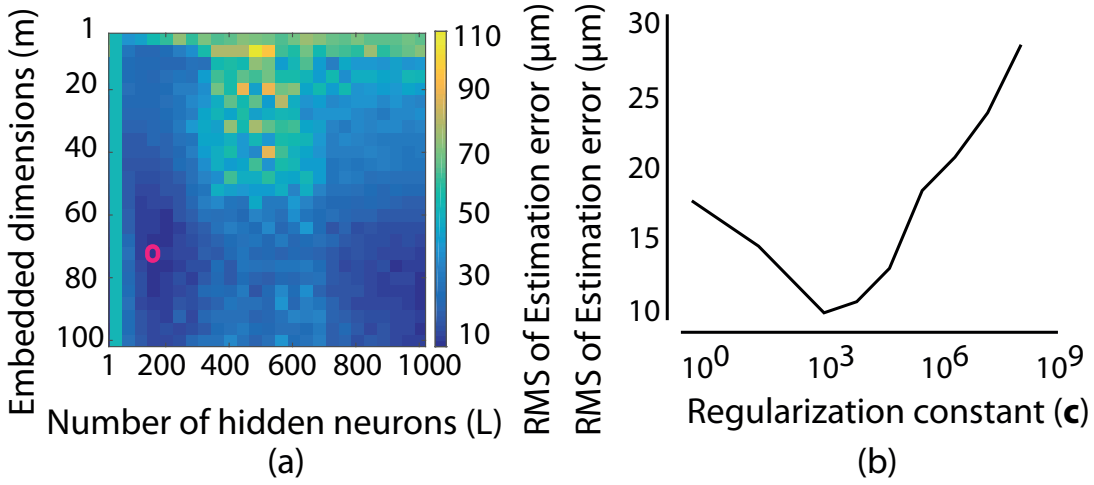

Figure 6: Optimal parameter selection for md-RELM a) grid search for L and m and b) optimal parameter for $\mathbf{c}$

3.5 Comparison analysis

In this section, comparisons analysis was conducted on tremor data set among 1) ELM (1D), 2) md-ELM, 3) md-RELM, 4) OS-mdRELM and 5) MWLSSVM (1D).

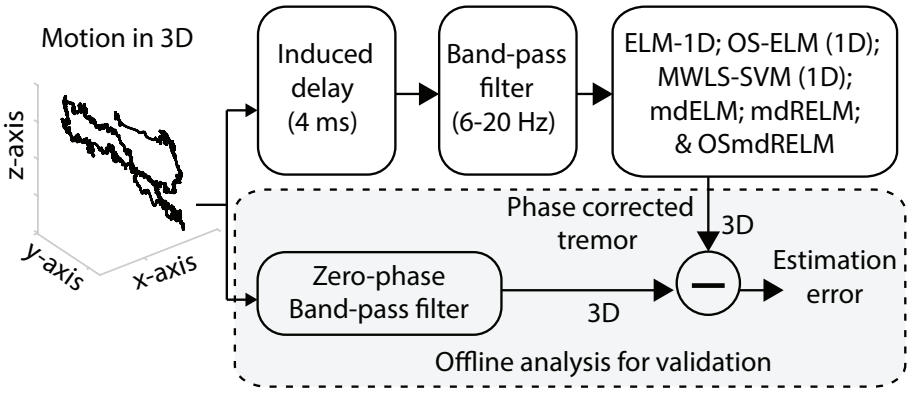

Figure 7: Phase delay correction

The procedure employed to validate each method is shown in Fig. 7. In this procedure, the 3D motion acquired with M2S2 system was provided to third-order Butterworth band-pass filter with pass-band of 6 to 20 Hz. As discussed earlier, this filtering stage introduces frequency dependent unknown phase delay into the procedure. The phase-distorted tremulous motion is provided to the devised phase-delay correction block to obtain in-phase tremulous motion. A zero-phase band pass filter with same specifications as above employed band-pass filter was employed to obtain the motion without any phase delay. This motion was employed as the ground truth to compare the performance of the phase-delay corrections, as shown in Fig. 7.

The multi-dimensional based phase-delay correction model with md-RELM was obtained with the training data set (first four seconds), as shown in Fig. 2. The parameters of md-RELM model were initialized as detailed in Section IIIC. The output weights obtained with the training dataset

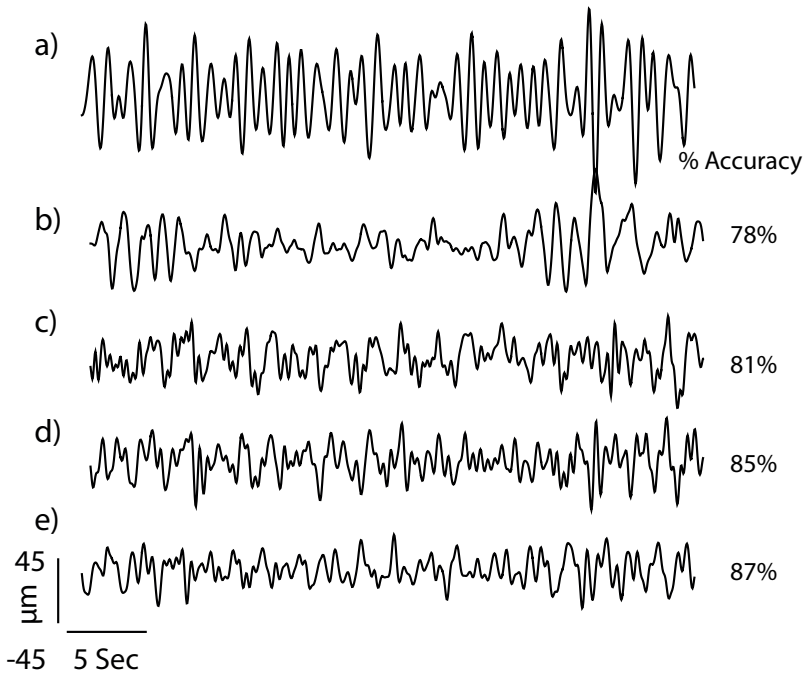

Figure 8: (a) Surgeon #1 (pointing task) (b) estimation error with ELM (c) estimation error with md-ELM (d) estimation error with md-RELM (e) estimation error with OS-mdRELM

for md-RELM were maintained throughout the testing data set. For the case of OS-mdELM, the phase-delay correction model updates at every available new sample to adapt to the time-varying phase-delay characteristics, as detailed in Section IIB.

The actual tremor motion in z-axis and estimation errors obtained with all methods on Surgeon #1 (pointing task) are provided in Fig. 8 for illustration. The estimation error obtained with single-dimensional ELM in Fig. 8(c) and multi-dimensional ELM in Fig. 8(d), highlights the influence of cross-dimension coupling in improving the performance. Further, the proposed md-RELM and OS-mdRELM demonstrates better performance compared to md-ELM and single-dimensional ELM.

To further quantify the performance of multi-dimensional approach, task-wise analysis was conducted on the whole database. As subjects require more control, they displayed huge variations in tremor amplitude while performing tracing task compared to the pointing task. Hence, the analysis was conducted separately for the two tasks. As pointing task is less complex compared to tracing task, *%accuracy* obtained for pointing task is higher than the *%accuracy* obtained with tracing task, as shown in Fig. 9. Over all subjects, multi-dimensional approach improved the tremulous motion filtering accuracy significantly. Among the methods, OS-mdRELM showed least estimation error. For pointing task, OS-mdRELM provided an average *%accuracy* of $83.87 \pm 1.93\%$ compared to $72.17 \pm 6.07\%$ and $69.74 \pm 11.32\%$ obtained with md-RELM and md-ELM respectively. On average of 9% improvement was obtained with the proposed multi-dimensional approach compared to the best existing single-dimensional approach MWLS-SVM.

To further highlight the improvement in modeling accuracy due to the incorporation of cross-dimensional coupling, a comparison analysis with OS-mdRELM is conducted for single-dimensional (1D), two-dimensional (2D), and 3D. For analysis, estimation of z axis is chosen as the output, whereas the input spaces are $\mathbf{s}_z(i)$, $\mathbf{s}_{x,z}(i)$ or $\mathbf{s}_{y,z}(i)$ and $\mathbf{s}_{x,y,z}(i)$ for 1D, 2D and 3D respectively.

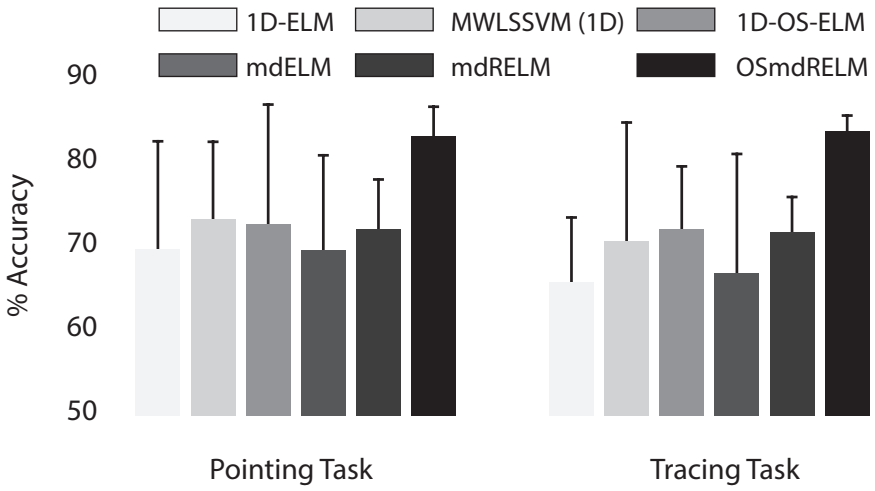

Figure 9: Performance analysis of all methods

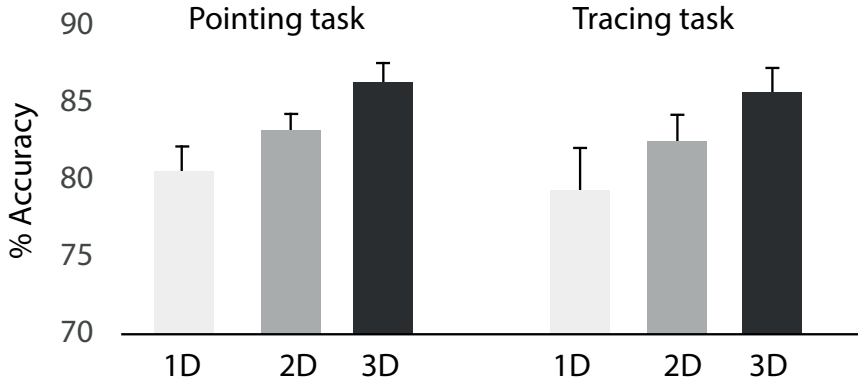

Figure 10: Performance analysis of OS-mdRELM for all dimensions

Results obtained for all subjects are shown in Fig. 10. An improvement of 3% accuracy can be seen in 3D compared to 2D for both the tasks. This also supports our hypothesis that cross-dimensional coupling improves the modeling accuracy.

3.6 Computation Complexity

Computational complexity plays a vital role in minimizing the delay in real-time implementation. The number of operations required for various existing methods and proposed methods are compared in Table. 1. Analysis shows that proposed methods computational complexity is similar compared to adaptive signal processing methods such as BMFLC-KF and significantly less compared to existing methods.

3.7 Experimental Validation

The experimental setup devised to validate the proposed multi-dimensional approach is shown in Fig. 11. In this setup, the surgical instrument was fixed on an anti-vibration table with an

Table 1: Computational complexity

Method	Parameters	Operations(O(·))
MWLSSVM [17]	$N = 1000$	$3 \times \mathcal{O}(N^3)$
MS-BMFLC-KF [10]	$n = 140$	$3 \times \mathcal{O}(n^3)$
md-ELM [21]	$L = 171$	$\mathcal{O}(L^3)$
md-RELM	$L = 171$, $n = 3$	$\mathcal{O}(L^3)$
OS-mdRELM	$L = 171$, $n = 3$	$\mathcal{O}(L^3) + \mathcal{O}(3L)$

angle of 45°. The subjects were asked to sit on a chair in a comfortable position and then rest their hand until wrist on the table, as shown in Fig. 11. The subjects were provided with the hand-held instrument (iTrem) and informed to hold the tip of hand-held instrument at the tip of the clamped surgical instrument for 50s. While performing the task, subjects were provided with a visual feedback through a table top optical surgical microscope (Leica M651 MSD, Leica Microsystem GmbH, Germany) with a built-in coaxial illuminator, as shown in Fig. 11. The magnification of the achromatic objective lens of the microscope is 25 and its focal length is 200 mm. For better view of the task performed, a zoom portion to the instrument tips is also shown in Fig. 11. The performed task was similar to the pointing task and a typical task in microsurgical procedures.

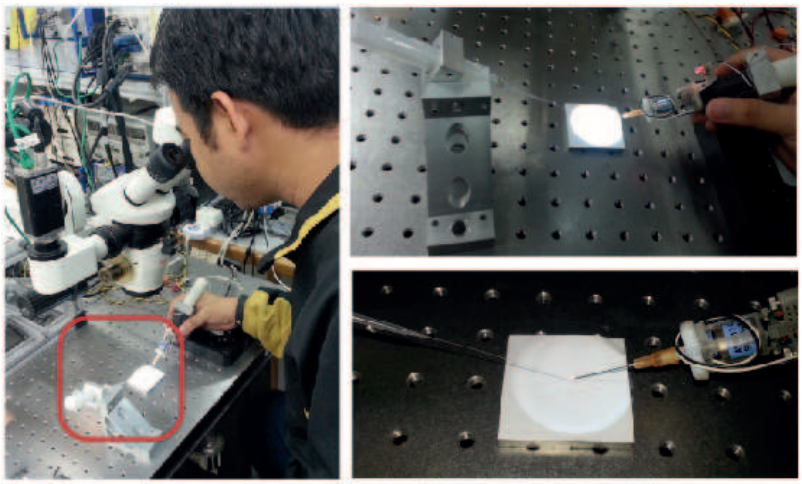

Figure 11: Experimental setup

The hand-held instrument (iTrem2) is housed with four dual-axis digital miniature MEMS accelerometers (ADIS 16003, Analog Devices, USA). The accelerometer measurements are acquired by the embedded micro-controller (AT89 C51CC03, Atmel, USA) on board iTrem2 at the sampling frequency of 333Hz. Real-time communication between iTrem2 and the real-time Labview environment was achieved by using the controller-area network (CAN) interface with a bandwidth of 500kbps. With a quadratic function, the acquired voltage readings from accelerometer were converted to acceleration and then converted into position domain with numerical integration in LabView environment [7]. The iTrem2 comprises of visual servo control integrated with inertial sensing to fulfill the need for hard real-timeliness in microsurgery (accurate sensing) [27]. The vision subsystem has a mono-vision camera mounted on the microscope which is located at a fixed position in the workspace. The camera gives the tool tip position information in X and Y axis;

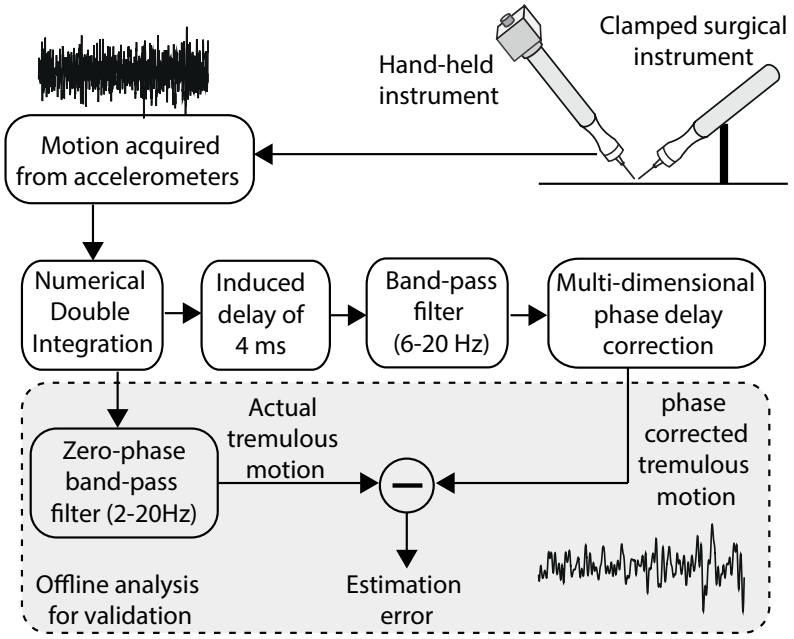

Figure 12: Experimental procedure for estimation of tremulous motion

it lacks the depth information (Z-axis). Thus, the setup is limited to 2-DOF in-plane movement with the instrument aligned with the microscope reference frame. For more details refer to [7, 27].

The procedure employed to evaluate the suitability of proposed multi-dimensional approach for tremor compensation is shown in Fig. 12. This approach is implemented as detailed in Fig. 3. The whole motion converted to position domain is provided to a band-pass filtering stage and then the proposed phase delay correction block, as shown in Fig. 12. The phase delay correction block is formulated according to the procedure detailed in Section. II. To evaluate the performance of the phase delay correction block, a zero-phase band pass filter was employed to provide the actual tremulous motion in offline (considered as ground truth). Further to account for the on-board first order low-pass filter in accelerometers (RC circuit with C = 10 μF and R = 40 $k\Omega$) and actuator delays, 4 ms delay block is also added to the signal as shown in Fig. 12. With the actual tremulous motion obtained in offline, estimation error was computed, as shown in Fig. 12.

Experiments were conducted with three subjects and three trials per each subject. Parameters and initial conditions for real-time experiments are similar to the simulation experiments. In [17], MWLS-SVM provided better performance compared to existing methods for multi-step prediction. Further based on our study in earlier section, we infer that md-RELM provides better performance compared to conventional ELM. Hence for experimental validation, we only choose OS-mdRELM, md-RELM and MWLS-SVM methods. For illustration, the estimation error obtained with OS-mdRELM and the estimation error due to the phase-delay for subject #1 are shown in Fig. 13. An $\%accuracy$ of 81%, 78%, and 74% were obtained with OS-mdRELM, md-RELM, and MWLS-SVM respectively. Overall for three subjects data, an average $\%accuracy$ of $79 \pm 1.23\%$ was obtained with OS-mdRELM, whereas $75 \pm 1.56\%$ and $71 \pm 1.89\%$ were obtained with md-RELM and MWLS-SVM respectively. Furthermore, OS-mdRELM provided better performance compared to all other method for all subjects and all trials.

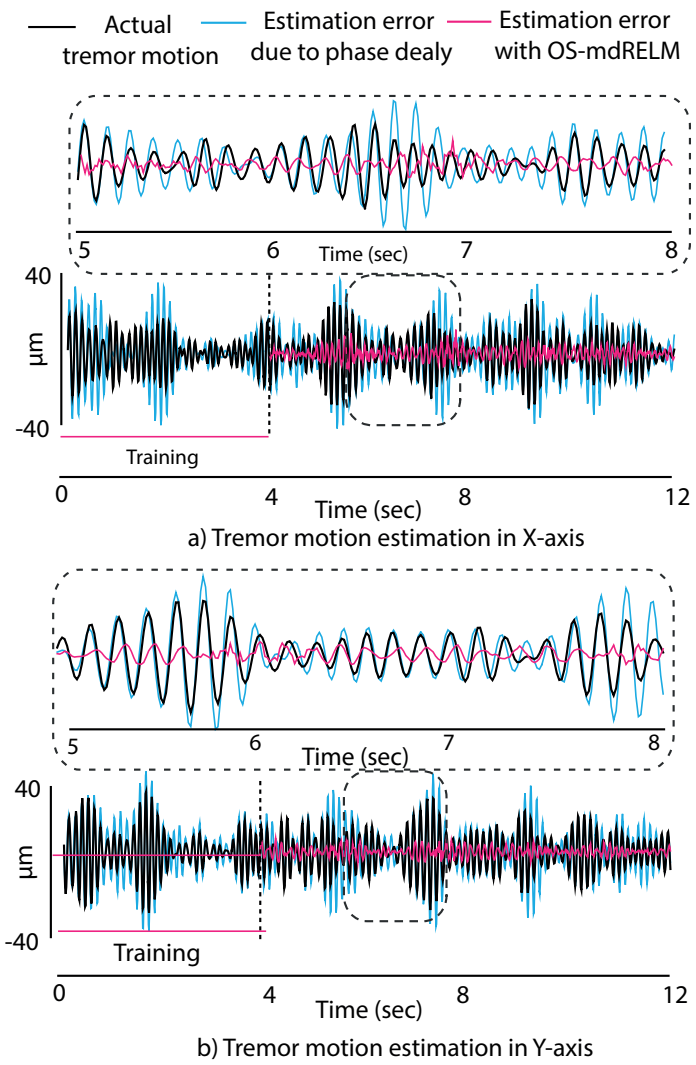

Figure 13: Experimental validation of OS-mdRELM

4 Discussions

The three-dimensional (3D) tremor estimation methods have been developed as a part of our continuing research to improve the performance of hand-held instruments. Correlation (linear relationship) and mutual information (nonlinear) are employed to analyze the existence of cross dimensional coupling in tremor measurements. To utilize this cross dimensional coupling information, embedded space with appropriate embedding dimensions ($m = 69$) and proper delay ($\tau = 1$) has been constructed with the data obtained from all three dimensions. The developed multi-dimensional modeling methods are trained in this embedded space to learn the nonlinear mapping that best represents the phase delay characteristics of a band pass filter, as shown in Fig. 2(b). It has been already established that if two time-series are correlated, then the information of one time series is included in the dynamics of other time-series. Consequently, the embedded space constructed with both time series better represents the geometry of time series rather than one time series alone [24, 25]. The reduction in prediction error with multi-dimensional methods

highlight that that there exists correlation across the dimensions and ELM has been successful in learning that. Furthermore, the proposed multi-dimensional modeling approaches are less computationally complex than other existing single-dimensional methods and are more suitable for active compensation in robotic systems.

Existing works on hand-held tremor compensation suggests that a final compensation of 70% is desirable for microsurgery to improve the surgeon's performance [7,8]. Analysis showed that the loss in end compensation accuracy was more due to phase delay, integration drift and other sensor noises. The proposed multi-dimensional approach improved the accuracy by nearly 10% compared to the existing methods. With this improvement, we foresee that the final compensation accuracy will be also improved during instrument trials will that are planned with micro surgeons in the future.

The hand-held instrument (iTrem2) employed in this work has a specially designed all-accelerometer inertial measurement unit to provide the instrument tool tip position in 3-DOF according to the fixed microscope reference frame [27]. Based on these measurements, the proposed multi-dimensional method has been customized to perform 3D tremor prediction. However, other variants of hand-held instruments, for example Micron [11] and steady hand [28], have incorporated 6-DOF (position and orientation) sensing units. Compared to 6-DOF sensing unit, the 3-DOF sensing based modeling lacks the information about the orientation. In recent work [29], it has been claimed that joint angle of wrist affects the physiological tremor. Thus, with 6-DOF modeling, the tremor modeling accuracy will be further improved. With the innate parallel processing structure of ELMs, the proposed multi-dimensional modeling (3-DOF) can be extended to 6-DOF modeling for other variants of hand-held instruments. However, the success of this extension to 6-DOF depends on accurate identification of the dependency across the six dimensions and the formulated of embedded space for learning.

Furthermore, to date, 3D tool tip control performance is applied to all three axes in parallel according to the generated control signal for each dimension separately. In other variants of hand-held instruments developed in [11] and [28], 6-DOF motion compensation have been developed. The combination of developed multi-dimensional modeling approaches with the 6-DOF compensation unit requires further work to be implemented in real-time. As a part of our continuing research in developing hand-held surgical instruments, we considered this exciting combination as our next step to work on.

Although the approach is mainly developed for 3D tremor modeling, the proposed approach is also suitable for 2D modeling as demonstrated in experiments. The significant improvement in modeling accuracy with 2D and 3D approaches further suggest that information available from other dimensions can significantly improve the modeling accuracy. The proposed multi-dimensional modeling can be successfully applied to 2D and 3D motion control problems [30, 31], bedsides the tremor modeling, with potential applications being precise 2D positioning with microscopes, mobility of robots, and cell manipulations and digital modeling of human motions.

5 Conclusions

As a solution to counter the unknown phase delay and perform simultaneous three-dimensional modeling of tremulous motion, multi-dimensional modeling with OS-mdRELM was developed in this paper. The analysis conducted on tremor data demonstrated that multi-dimensional methods

provide better tremor estimation compared to other methods. To evaluate the suitability of multi-dimensional approach for real-time applications, the approach was evaluated experimentally in comparison with existing methods. Results show that an average $\%Accuracy$ of $79 \pm 1.23\%$ is obtained with the OS-mdRELM in comparison to $71 \pm 1.89\%$ obtained with the existing method MWLS-SVM (1D).

References

[1] M. Patkin, "Ergonomics applied to the practice of microsurgery," *Aust. N.Z. J. Surg.*, vol. 47, no. 3, pp. 320–329, Jun. 1977.

[2] R. J. Elbe and W. C. Koller, *Tremor*, U. MD, Ed. John Hopkins University Press: Baltimore, MD, USA, 1985.

[3] G. Deuschl, J. Raethjen, and M. Lindemann, "The pathophysiology of tremor," *Muscle & Nerve*, vol. 24, no. 6, pp. 716–735, Jun. 2001.

[4] D. B. Camarillo, T. M. Krummel, and J. K. Salisbury, "Robotic technology in surgery: past, present, and future," *Am. J. Surg.*, vol. 188, no. 4, pp. 2S–15S, Oct. 2004.

[5] C. J. Payne and G. Z. Yang, "Hand-held medical robots," *Ann. Biomed. Eng.*, vol. 42, no. 8, pp. 1594–1605, Aug. 2014.

[6] W. T. Ang, C. N. Riviere, and P. K. Khosla, "An active hand-held instrument for enhanced microsurgical accuracy," in *Medical Image Computing and Computer-Assisted Intervention – MICCAI 2000*, S. L. Delp, A. M. DiGoia, and B. Jaramaz, Eds. Springer Berlin Heidelberg, Oct. 2000, pp. 878–886.

[7] W. T. Latt, U. X. Tan, C. Y. Shee, C. N. Riviere, and W. T. Ang, "Compact sensing design of a handheld active tremor compensation instrument," *IEEE Sens. J.*, vol. 9, no. 12, pp. 1864–1871, Dec. 2009.

[8] C. N. Riviere, W. T. Ang, and P. K. Khosla, "Toward active tremor canceling in handheld microsurgical instruments," *IEEE Trans. Robot. Auto.*, vol. 19, no. 5, pp. 793–800, Oct. 2003.

[9] K. A. Mann, F. W. Werner, and A. K. Palmer, "Frequency spectrum analysis of wrist motion for activities of daily living," *J. Orthop. Res.*, vol. 7, no. 2, pp. 304–306, Mar. 1989.

[10] K. C. Veluvolu, S. Tatinati, S. M. Hong, and W. T. Ang, "Multistep prediction of physiological tremor for surgical robotic applications," *IEEE Trans. Biomed. Eng.*, vol. 60, no. 11, pp. 3074–3082, Nov. 2013.

[11] R. A. MacLachlan, B. C. Becker, J. C. Tabares, G. W. Podnar, L. A. Lobes, and C. N. Riviere, "Micron : An actively stablized handheld tool for microsurgery," *IEEE Trans. Robot.*, vol. 28, no. 1, pp. 195–212, Feb. 2012.

[12] K. C. Veluvolu and W. T. Ang, "Estimation and filtering of physiological tremor for real-time compensation in surgical robotics applications," *Int. J. Med. Robot. Comput. Assist. Surg.*, vol. 6, no. 3, pp. 334–342, Sept. 2010.

[13] K. C. Veluvolu, Y. Wang, and S. Kavuri, "Adaptive estimation of EEG rhythms for optimal band estimation in BCI," *J. Neurosci. Methods*, vol. 203, no. 1, pp. 163–172, Jan. 2012.

[14] Y. Wang, K. C. Veluvolu, J. H. Cho, and M. Deforrt, "Adaptive estimation of EEG mu-rhythm for subject-specific reactive band identification and improved ERD detection," *Neurosci. Lett.*, vol. 528, no. 2, pp. 137–142, Oct. 2012.

[15] K. Adhikari, S. Tatinati, W. T. Ang, K. C. Veluvolu, and K. Nazarpour "A quaternion weighted Fourier linear combiner for modeling physiological tremors," *IEEE Trans. Biomed. Eng.*, 2016, In Press.

[16] S. Tatinati, K. C. Veluvolu, S. M. Hong, W. T. Latt, and W. T. Ang, "Physiological tremor estimation with autoregressive (AR) model and Kalman filter for robotic applications," *IEEE Sens. J.*, vol. 13, no. 12, pp. 4977 – 4985, Dec. 2013.

[17] S. Tatinati, K. C. Veluvolu, and W. T. Ang, "Multi-step prediction of physiological tremor based on machine learning for robotics assisted microsurgery," *IEEE Tran. Cybern.*, vol. 45, no. 2, pp. 328–338, Feb. 2015.

[18] A. Shilton, D. T. H. Lai, and M. Palaniswami, "A division algebraic framework for multidimensional support vector regression," *IEEE Trans. Syst. Man. Cybern. B Cybern.*, vol. 40, no. 2, pp. 517–528, Apr. 2010.

[19] W. Mao, S. Zhao, X. Mu, and H. Wang, "Multi-dimensional extreme learning machine," *Neurocomputing*, vol. 149, pp. 160–170, Feb. 2015.

[20] H. T. Huynh and Y. Won, "Regularized online sequential learning algorithm for single-hidden layer feed-forward neural network," *Pattern Recognition Letters*, vol. 32, no. 14, pp. 1930–1935, Oct. 2011.

[21] G. B. Huang, H. Zhou, X. Ding, and R. Zhang, "Extreme learning machine for regression and multiclass classification," *IEEE Trans. Syst. Man. Cybern. B Cybern.*, vol. 42, no. 2, pp. 513–529, Aor. 2012.

[22] G. Huang, G. B. Huang, S. Song, and K. You, "Trends in extreme learning machine: A review," *Neural Netw.*, vol. 61, no. 1, pp. 32–48, Jan. 2015.

[23] N. Y. Liang, G. B. Huang, P. Saratchandran, and N. Sundararajan, "A fast and accurate online sequential learning algorithm for feedforward networks," *IEEE Trans. Neural Netw.*, vol. 17, no. 6, pp. 1411–1423, Nov. 2006.

[24] H. S. Kim, R. Eykhlot, and J. D. Salas, "Nonlinear dynamics, delay times, and embedding windows," *Physica D*, vol. 127, no. 1-2, pp. 48–60, Mar. 1999.

[25] T. Schreiber, "Measuring information transfer," *Phys. Rev. Lett.*, vol. 80, no. 2, pp. 461–464, Jul. 2000.

[26] L. M. S. Eileen, W. T. Latt, W. T. Ang, T. C. Lim, C. L. Teo, and E. Burdet, "Micromanipulation accuracy in pointing and tracing investigated with a contact-free measurement system," in *Conf. Proc. IEEE Eng. Med. Biol. Soc.*, Sept. 2009, pp. 3960–3963.

[27] Y. N. Aye, S. Zhao, and W. T. Ang, "An enhanced intelligent handheld instrument with visual servo control for 2-DOF hand motion error compensation," *Int. J. Adv. Robot. Syst.*, vol. 10, pp. 1–8, Oct. 2013.

[28] B. Mitchell, J. Koo, I. Iordachita, P. Kazanzides, A. Kapoor, J. Handa, G. Hager, and R. Taylor, "Development and application of a new steady hand manipulator for retinal surgery," in *IEEE Int. Conf. Robot Autom.*, Apr. 2007, pp. 623–629.

[29] B. Carignana, J. F. Daneault, and C. Duval, "The effect of changes in joint angle on the characteristics of physiological tremor," *J. Electromyogr. Kinesiol.*, vol. 22, no. 6, pp. 594–960, Dec. 2012.

[30] Y. Jiang, K. Yang, C. Hu, and D. Yu, "A data-driven iterative decoupling feed forward control strategy with application to an ultra precision motion stage," *IEEE Trans. Ind. Electron.*, vol. 62, no. 1, pp. 620–627, Jan. 2015.

[31] S. Y. Shin and C. H. Kim, "Human-like motion generation and control for humanoids dual arm object manipulation," *IEEE Trans. Ind. Electron.*, vol. 62, no. 4, pp. 2265–2276, Apr. 2015.

Sivanagaraja Tatinati received the Masters and PhD degrees in electronics engineering from Kyungpook National University, Daegu, South Korea. He is currently working as a post-doctroal fellow at school of Computer Science and Engineering, Kyungpook National University, Daegu, South Korea. His current research interests include robotics-assisted medical instruments, adaptive filtering, machine learning techniques based regression with applications in bio-medical engineering.

Kianoush Nazarpour(S'05-M'08-SM'14) received the B.Sc. degree from K. N. Toosi University of Technology, Tehran, Iran, in 2003, the M.Sc. degree from Tarbiat Modarres University, Tehran, Iran, in 2005, and the Ph.D. degree from Cardiff University, Cardiff, U.K., in 2008, all in electrical and electronic engineering. From 2007 to 2012, he held two Postdoctoral

Researcher posts at Birmingham and Newcastle Universities. In 2012, he joined Touch Bionics, Inc., U.K., as a Senior Algorithm Engineer working on intelligent control of multifunctional myoelectric prostheses. In 2013, he returned to Newcastle University, where he is currently a Senior Lecturer in biomedical engineering. His research interests include intelligent sensing and biomedical signal processing and their applications in assistive technology. Dr. Nazarpour received the Best Paper Award at the 3rd International BrainComputer Interface (BCI) Conference (Graz, Austria, 2006), and the David Douglas Award (2006), U.K., for his work on joint spacetime frequency analysis of the electroencephalogram signals. He is currently an Associate Editor of the Medical Engineering and Physics journal in the area of biomedical signal processing.

Wei Tech Ang(S'98-M'04) received the B.E. and M.E. degrees in mechanical and production engineering from Nanyang Technological University, Singapore, in 1997 and 1999, respectively, and the Ph.D. degree in robotics from Carnegie Mellon University, Pittsburgh, PA, USA, in 2004. Since 2004, he has been with the School of Mechanical and Aerospace Engineering, Nanyang Technological University, where he is currently an Associate Professor and holds the appointment of Head of Engineering Mechanics Division. His research focuses on robotics technology for Biomedical applications, which include surgery, rehabilitation and cell micromanipulation.

Kalyana C. Veluvolu(S'03-M'06-SM'13) received the B.Tech. degree in electrical and electronic engineering from Acharya Nagarjuna University, Guntur, India, in 2002, and the Ph.D. degree in electrical engineering from Nanyang Technological University, Singapore, in 2006. During 2006-2009, he was a Research Fellow with the Biorobotics Group, Robotics Research Center, Nanyang Technological University. Since 2009, he has been with the School of Electronics Engineering, Kyungpook National University, Daegu, Korea, where he is currently an Associate Professor. He is also currently attached to the school of mechanical and aerospace engineering, Nanyang Technological University, Singapore as a visiting professor for period 2016-2017. He has been a Principal Investigator or a Co investigator on a number of research grants funded by the National Research Foundation of Korea, and other agencies. He has authored or coauthored over 100 journal articles and conference proceedings. His current research interests include nonlinear estimation and filtering, sliding mode control, brain-computer interface, autonomous vehicles, biomedical signal processing, and surgical robotics.